Finite Elements in Analysis and Design 116 (2016) 1–11

Contents lists available at ScienceDirect

Finite Elements in Analysis and Design

journal homepage: www.elsevier.com/locate/finel

Vibrational modes of multilayered ceramic capacitors ☆

Kirsten L. Peterson [a,*], Ward L. Johnson [b], Sudook A. Kim [b], Paul R. Heyliger [a]

[a] Department of Civil and Environmental Engineering, Colorado State University, Fort Collins, CO 80523, United States
[b] Applied Chemicals and Materials Division, National Institute of Standards and Technology, 325 Broadway St., Boulder, CO 80305, United States

ARTICLE INFO

Article history:
Received 2 October 2015
Received in revised form
11 March 2016
Accepted 27 March 2016
Available online 28 April 2016

Keywords:
Multilayer ceramic capacitors
Finite element modeling
Vibrational modes
Resonant acoustics

ABSTRACT

Micron-scale spacing of interleaved electrodes and high-dielectric ceramics in multilayer ceramic capacitors (MLCCs) provide exceptionally high capacitances in small volumes. This has led to MLCCs being the preferred type of capacitor in a wide range of applications where size and weight are critical factors. However, crack-related failures of MLCCs remain a significant issue. Resonant ultrasound spectroscopy (RUS) and resonant nonlinear ultrasonics are being pursued as nondestructive techniques for detecting subsurface cracks that can evolve into performance-degrading electrical pathways during service. This paper presents finite-element calculations of the vibrational modes of MLCCs. The geometric symmetry in the finite-element model was orthorhombic, with three orthogonal mirror planes, and the detailed internal structure of interleaved metallic and ceramic materials was included in the model. The assumption of three mirror planes enabled an analysis of the normal modes of the full model through calculations on a mesh spanning just one eighth of the full volume. The computational load was further reduced by separating the problem into eight modal-symmetry sets with different boundary conditions for each set. The first three non-zero frequencies are presented for each modal symmetry set. In addition, displacement plots are presented for the two or three lowest-frequency modes of each symmetry set. These results provide information on the frequency ordering and symmetries of vibrational modes that can be used in the analysis of ultrasonic resonance measurements of MLCCs.

1. Introduction

The development and commercialization of multilayer ceramic capacitors (MLCCs) has been a significant factor leading to reductions in size of a wide variety of electrical circuits, because the micron-scale spacing of interleaved electrodes and high-dielectric ceramics in MLCCs provides exceptionally high capacitance in small volumes. However, there are challenges with enhancing the reliability of MLCCs associated with the intrinsic vulnerability of the dielectric ceramic material to cracking under stress during manufacture, soldering, and service [1]. Although relatively rare, crack-related failures of MLCCs remain a significant issue, especially in applications where the repercussions of failure can be catastrophic or replacement is impossible, costly, or dangerous, as in implantable medical devices and spacecraft.

Established methods for screening MLCCs for flaws before and after their incorporation in electrical circuits include visual inspection and measurements of electrical leakage current [1]. However, these methods are ineffective at detecting the presence of subsurface cracks that can evolve into performance-degrading electrical pathways during service [1–3]. This situation has motivated research on acoustic inspection methods that are sensitive to internal structure. Such research has included work on scanning acoustic microscopy, scanning laser acoustic microscopy, resonant ultrasound spectroscopy (RUS), electromechanical resonance spectroscopy employing swept-frequency impedance analysers, and tone-burst electromechanical resonance [2–10].

Two published studies of MLCCs have included finite-element (FE) modeling of resonant vibrational modes to support the interpretation of experimental spectra [6,9]. Prume et al. [6] calculated FE impedance spectra with piezoelectric and dielectric terms included in the equation of motion and the excitation provided through direct ferroelectric coupling to electric fields applied to the internal interleaved electrodes. The transduction mechanism in this model and corresponding impedance measurements introduces restrictions on the excited modal symmetries. Capacitors with industrial size designations of 1210 and 1812 were included in these models, and the effects of delaminations and idealized cracks with two different orientations were explored through comparisons of calculated and experimental spectra. Johnson et al. [9] reported FE normal-mode spectra and displacement patterns for several resonant modes near the dominant experimentally measured resonant peaks of smaller type-0603

☆This manuscript is a contribution of the National Institute of Standards and Technology and is not subject to copyright in the United States.

* Corresponding author.
E-mail address: kirstenpeterson999@gmail.com (K.L. Peterson).

http://dx.doi.org/10.1016/j.finel.2016.03.002
0168-874X/

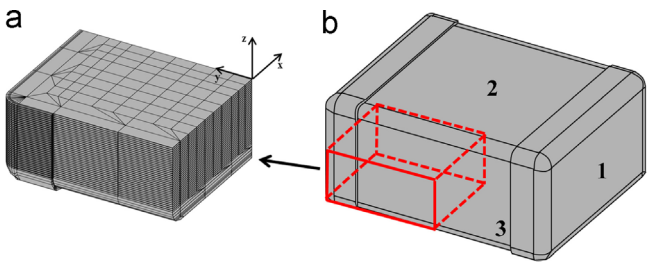

Fig. 1. (a) Magnified view of the single octant that is meshed and analyzed in the finite-element calculation and (b) geometry of the entire capacitor. The metal endcaps of the capacitor appear as raised areas with rounded edges. The darker grey regions in (a) represent the finely interleaved layers of ceramic and metallic electrodes with their largest surfaces in the x–y plane. Surface labels are defined in (b) as 1, 2, and 3.

MLCCs driven with ferroelectric excitation. The FE model in that study did not include ferroelectric excitation or piezoelectric/dielectric terms in the equation of motion.

The current paper presents FE calculations of acoustic normal modes of all symmetry types, based on an MLCC model with dimensions and internal structure approximately matching those previously reported for a set of type-1210 MLCCs [10]. Internal interleaved layers of electrodes and ceramic are explicitly included in the model, although the geometry of these layers is approximated as orthorhombic to reduce the size of the computational problem (as in the work of Prume et al. [6]). Piezoelectric and dielectric terms are not included in the equation of motion. The inclusion of all modal symmetries in the model is anticipated to facilitate interpretation of RUS measurements, which are not limited to excitation of specific symmetries. The research reported here is specifically associated with experimental work that has been reported elsewhere on the detection of cracks in MLCCs through RUS [8] and tone-burst electromechanical resonance [10].

2. The capacitor

2.1. Geometry

The geometry in the FE model considered here is shown in Fig. 1 and is based on measurements reported by Johnson et al. [10] for a set of type-1210 MLCCs manufactured by Vishay Intertechnology with model number of VJ1210Y474KXAAT.[1]

The three exterior surfaces of the capacitor shown in Fig. 1(b) are defined for the purpose of describing the displacement pattern results. The endcap surface (with surface-normal vector in the $\hat{y}$ direction) is Surface 1, the larger capacitor surface (with surface-normal vector in the $\hat{z}$ direction) is Surface 2, and the smaller capacitor surface (with surface-normal vector in the $\hat{x}$ direction) is Surface 3. As described by Johnson et al. [10], the 70 electrodes in the core of the physical MLCC have a thickness of 2.0 μm and a periodicity of 16.38 μm, corresponding to a total thickness of 1.132 mm for the interleaved core region. The width and length of the internal electrodes are 2.068 mm and 2.852 mm, respectively, and connect alternately to the two metallic endcaps of the MLCC. The electrodes are surrounded by a ceramic filler material (a typical dielectric for MLCCs described in a subsequent section) with overall dimensions of 2.474 mm, 3.040 mm, and 1.414 mm. The endcaps each consist of three metallic layers. The thicknesses of the metallic layers from outside to inside (tin, nickel, and silver, respectively) are 15.0 μm, 9.0 μm, and 7.0 μm, for a total summed thickness on one end of 31.0 μm, resulting in final overall dimensions of 2.536 mm, 3.102 mm, and 1.476 mm in the $\hat{x}$, $\hat{y}$, and $\hat{z}$ directions, respectively, shown in Fig. 1.

The nominal symmetry of the physical MLCCs is monoclinic (corresponding to the group-theoretical point group C_{2h} in the Schoenflies notation), with one mirror plane ($y-z$) and a two-fold rotation axis ($\hat{x}$) normal to this plane [11]. The exterior surfaces of the physical MLCC, as depicted in Fig. 1(b), have a higher symmetry corresponding the orthorhombic point group D_{2h}, with three mirror planes and corresponding two-fold rotation axes and inversion symmetry [11]. The reduced symmetry of the full capacitor arises from the fact that alternating connections of the even number of internal electrodes to the endcaps eliminates two of the mirror planes. In this study, this reduction in symmetry of the physical MLCC is neglected, and the total symmetry of the capacitor is approximated as D_{2h}. This approximation of higher symmetry is implemented in the model by having the electrodes in the model alternately connect to either both endcaps or neither endcap, rather than alternately to one or the other endcap as in the physical capacitor. This is equivalent to shifting the location of a portion of the internal electrode material near the endcaps by one period (16.38 μm) of the interleaved structure. The effect of this approximation is expected to be insignificant because (1) it shifts the position of electrode material by only a small fraction of the exterior dimensions, (2) it does not change the relative volumes of the materials in the capacitor and (3) it does not lead to an introduction or splitting of degenerate modes, because there are no degeneracies in either the C_{2h} or the D_{2h} point groups. Also, the thicknesses of the ceramic material above and below the core region of the physical MLCCs can vary from capacitor to capacitor. For simplicity, it was assumed for the mesh that the x–y midplane falls exactly between two layers. Therefore, because the mesh assumes symmetry across the x–y reflection plane, an electrode with double the thickness appears at the very center of the mesh, and this feature does not exist in the physical MLCC. Again, because this assumption does not change the volume fraction of the materials, it is a useful approximation that significantly reduces the size of the computational problem.

The D_{2h} symmetry of the model enables the FE calculations to be performed on only one octant of the MLCC (as shown in Fig. 1), with boundary conditions specified to match the specified modal symmetries. This resulted in a mesh with 75 total layers of elements in the $\hat{z}$ direction within the octant. The curved bottom ceramic region was modeled with 5 layers of elements through the thickness. Each pair of electrode and ceramic layers (every 16.38 μm) was modeled with two elements through the thickness, resulting in 70 total layers of elements for the core region, 35 including both dielectric and electrode materials and 35 with only dielectric material. As described below, the endcaps have a relatively small effect on the frequencies. Therefore, highly exact modeling of the endcaps is assumed not to be critical, and, to save on computational time, the endcaps were modeled with only one element through the thickness of each metallic endcap layer. The capacitor octant mesh has overall dimensions of 1.268 mm, 1.551 mm, and 0.738 mm in the $\hat{x}$, $\hat{y}$, and $\hat{z}$ directions, respectively. These values are half of the overall dimensions given for the whole capacitor. A generally square mesh was implemented for the layers, with the corners modeled with triangular wedge elements extending radially. This mesh geometry is shown in Fig. 1. A convergence study to determine the appropriate refinement of this core region of the mesh is described in a subsequent section. Triangular wedge elements were also used to connect the coarser portion of the mesh for the curved bottom ceramic region with the refined core region. The origin of the coordinate system is located at the center of the full capacitor. The total volume of the meshed octant (one eighth of entire capacitor) is 1.369×10^{-9} m^3.

[1] Identification of this commercial product is provided for technical completeness and does not reflect an endorsement by NIST.